Noise removal using adaptive filtering for ultrasonic guided wave testing of pipelines

Houman Nakhli Mahal
Brunel University London, Uxbridge, Kingstone Lane, London, UB8 3PH
Houman.nakhlimahal@brunel.ac.uk

Peter Mudge,
TWI, Granta Park, Great Abington, CB21 6AL

Asoke K. Nandi,
Brunel University London, Uxbridge, Kingstone Lane, London, UB8 3PH

Abstract

One of the most recent technologies for NDT of pipelines is Ultrasonic Guided Waves (UGW), using low-frequency ultrasound signals to enable long-range inspection. In inspection, the practice is to excite a pure single axisymmetric wave mode in their non-dispersive region. Due to mode conversion and impure testing condition, various other wave modes exist in the received waveforms. To find the defect location, one needs to be able to identify the axisymmetric wave mode from this coherent noise in the signal. Due to the variability of coherent noise, there is a need for a procedure to update adaptively with regard to the local characteristic of the received signals. Adaptive filtering is a powerful tool in removing time-varying additive noise from the coherent signals of interests in the observations and is able to achieve higher Signal-to-Noise Ratio (SNR). In this paper, a strategy is provided to use adaptive leaky filters and is validated by using laboratory trials on an experimental pipe which resulted in significant increment of SNR.

1   Introduction

Ultrasonic Guided Wave (UGW) allows long-range Non-Destructive Testing (NDT) of pipes from a single point of inspection. This technology uses several collars (depending on the device), installed on the circumference of a pipe. Each of these collars includes many transducers which are operating in pulse-echo mode. One of the main problems of UGWs is that they are inherently multimodal and dispersive. In general inspection of pipelines, pure axially-symmetric (axisymmetric) modes, Torsional and Longitudinal, in their non-dispersive regions are used to decrease the complexity in the interoperation of the results. Guided-wave propagation routine produces a single signal in the time-domain for inspectors. The defects are then detected based on Signal-to-Noise (SNR) ratio, where an anomaly is reported if the signal envelope is higher than the regional noise level [1].

This propagation routine signal is generated by summing the phase-delayed version of the received signal of each transducer. The phase-delay operation is dependent on the excitation wave mode and frequency, ring-spacing of the device and the test direction [2], [3]. The physics of guided-waves allowed us to use this method to remove the zero-mean flexural waves by linearly placing the transducers on circumference and achieve test unidirectionality by supressing the excited wave form using their dispersion curves. Various approaches have been tried in the literature for improving the SNR. One of the methods is to use pulse-compression [3]–[6]. However, this technique requires the design of an excitation waveform and the performance and the design of optimum excitation sequence can be dependable on the testing condition such as the transfer functions of the transducer. On the other hand, filtering approaches such as Split-Spectrum Processing have also been implemented. In 2018, Pedram et al. [7] utilised Split-Spectrum Processing to enhance the SNR of tests. While significant improvements can be achieved in this way, the algorithm depends on many different parameters and the results could be changed on a case by case basis. Most of the methods in the literature consider the signals achieved after the devices propagation routine as the main input signals of their implemented techniques. Nonetheless, the device inherently produces a multidimensional signal.

The main aim of this paper is to utilise the multi-dimensionality of the device signals in order to increase the SNR. Adaptive filtering is implemented to reduce the effect of coherent noise of the tests. Synthesised data are used for quantitively assessing the performance of this technique. The results demonstrate a significant improvement of SNR compared to the results generated from general propagation routine.

2 Background

Guided-waves exhibit dispersive propagation, which causes the energy of a signal to spread out in space and time as it propagates [8]. Figure 1 shows an arbitrary created example of a dispersive flexural wave where the black lines are showing the signal after 1 meter of propagation and red lines are showing the same wave, after 2 meters of propagation. As can be seen, the energy of the wave is spreading in time decreasing the temporal resolution and the amplitude of the wave. For ease of inspection, *T(0,1)* wave mode, which is a non-dispersive across the whole frequency range, is used [9].
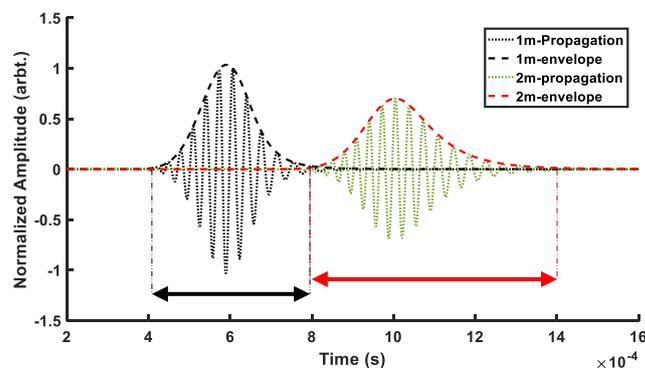

Figure 1: Arbitrary example of dispersive propagation of F(4,2) wave propagating in a pipe at two distances of 1m and 2m. wave 30khz, 10 Cylce, Hann windowed sine wave.

Furthermore, guided waves are multimodal [10] and the wave modes are categorized based on their displacement patterns (mode shapes) within the structure. The main categories of guided waves in pipes are axisymmetric Torsional and Longitudinal waves, and non-axisymmetric Flexural waves. The popular nomenclature used for them are in the format of $X(n,m)$, where X can be replaced by letters L for Longitudinal, T for Torsional, and F for flexural waves, n shows the harmonic variations of displacement and stress around the circumference, and m represents the order of existence of the wave mode [11]. A single pure family of axisymmetric waves should be generated in their non-dispersive region should be excited for the general inspection. However, due to the device imperfections in real-life scenarios and mode conversion from the impact of axisymmetric waves with the features within structures, the received signal contains a mixture of excited axisymmetric and flexural waves. [10], [12], [13]. In order to reduce the flexural waves, arrays of transducers have to be placed equally spaced around the circumference of the pipe. To create mono-directionality, multiple arrays/rings of transducers have to be used. Backward propagating wave can be cancelled by phase delaying and inverse the signal from the first array with regards to the excitation frequency and the distance between two arrays [3].

Figure 2 shows the spatial arrival of the signals from different segments of the pipe. These signals are created using the model in [14], where a three ring excitation system is used. Each ring contains 32 source points with variable transfer functions. Doing so ensures the generation of coherent noises with same characteristics as the real testing condition. In the polar plots, blue and red lines represent two circumferential rings while the black dotted line serves as the reference; thus, points inside the circle representing negative displacements and those above the circle are showing positive displacement in that section of the pipe. The following can be concluded:

- The energy of the received waves from axisymmetric features such as pipe end are overwhelmed by the $T(0,1)$ with little variances caused by the Flexurals.
- Defect signals have a mixture of both Flexurals and Torsional wave modes; nonetheless, for wide Cross-Sectional Area (CSA) loss, $T(0,1)$ will have greater energy than the Flexurals.
- Noise regions are overwhelmed by the Flexurals with almost no axisymmetric wave being detected. For these regions, the resultant signal from in two rings can be highly variable since it depends on the spatial shape of the wave modes.
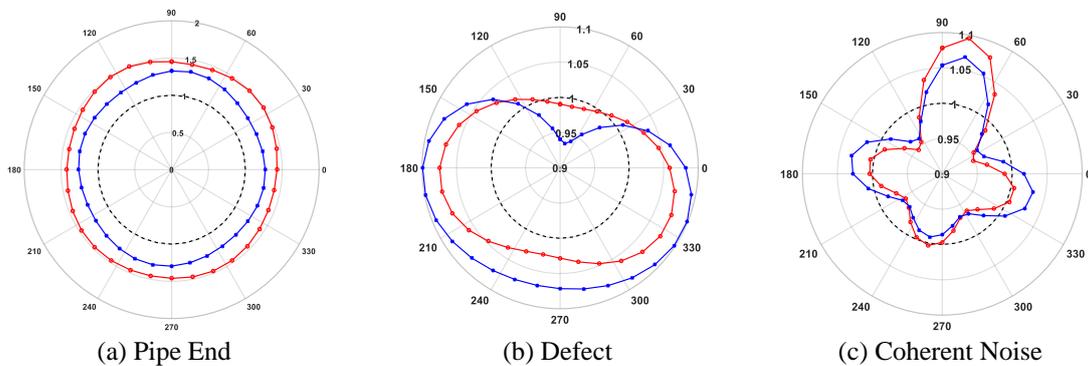

(a) Pipe End   (b) Defect   (c) Coherent Noise

Figure 2: Example signals from the array from different sections of a pipe (FEA).

Three main signals are expected to be received in guided-wave tests which are shown in Figure 3. The first signal is the superposing of $T(0,1)$ and Flexurals where it is the true defect location. The second is the Flexurals created due to wave mode conversion [15]; as these signals exhibit the same characteristics of the excitation waveform, they can lead to detection of false alarms. The third category is the non-coherent white noise which are not correlated to the excitation sequence.
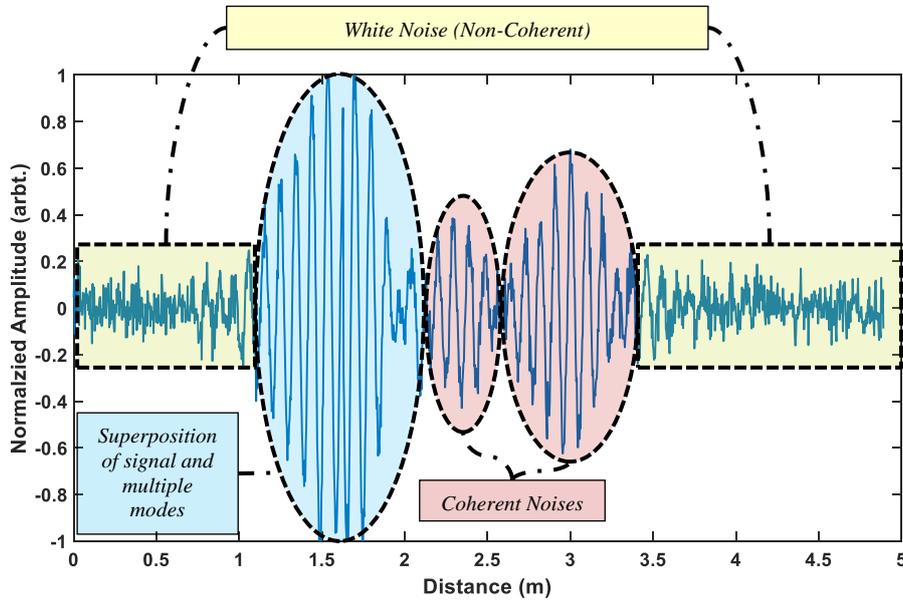

Figure 3: Categories of noise in guided-wave inspection.

2.1 Test Setup

For the purposes of technique development, synthetic signals created by Finite-Element-Analysis (FEA) model and real laboratory pipes are used. The pipe is modelled based on the standard 8" schedule 40 steel pipe characteristics, with a length of 6 m, outer-diameter of 219.1 mm and thickness of 8.18 mm, Young's Modulus of 210 GPa, Density of 7850-kg/m^3 and Poisson's Ratio of 0.3 is used. The model is created in ABAQUS Software [16], where a defect is located 3 meter away from the test point [14]. Two main signals are expected to be received in the front propagation which are located at 3 m and 4 m as shown in Figure 4. The second signal is the result scattering result of backward leakage with defect located in the front which happens due to the variable transfer functions.
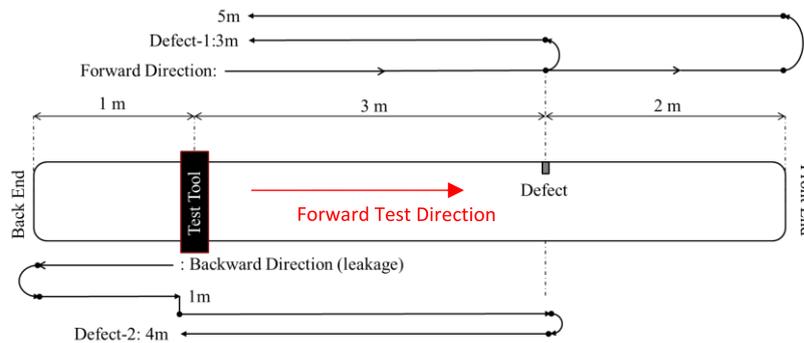

Figure 4: Torsional Mode signal reception routes in the FEA test case.

3   Signal Processing

In the field of signal processing, filtering is one of the common and important processes [17]. The key component of an adaptive filter is to define filter updates in a way that decreases the mean-square error between the reference and response iteratively. One of the robust methods is the normalized least mean square [18]–[21], that tries to minimize the least mean square error by setting the coefficients according to a variable step-size. Also, a forgetting factor α allows the filter to be adjusted quicker to the characteristics of the current iteration. The used updating formula for filter values is as follows:

$$w_{n+1} = \alpha w_n + \beta \frac{x'(n)}{\epsilon + |x(n)|^2} e(n) \tag{1}$$

where w is the filter weight, β is the normalized-step size, ϵ is the compensation factor, $x(n)$ and $e(n)$ are representing the input and error signal of the adaptive filter respectively. The flow chart for using adaptive filters in noise-cancellation is shown in Figure 5. In this setup, instead of adding the signals received from the rings of transducers, they are selected as the desired response $d(n)$, and the input signal $x(n)$. Every other signal is updated based on the characteristics within each iteration and $y(n)$ is the output of the filter.
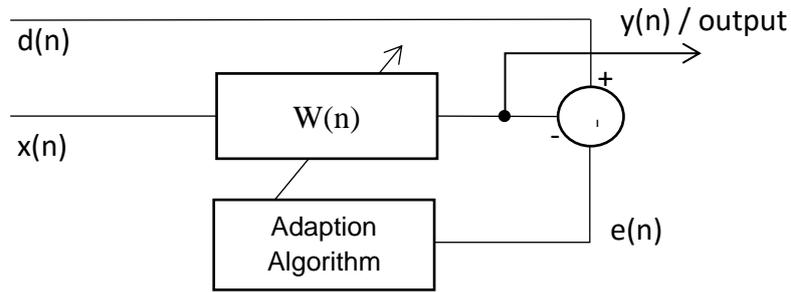

Figure 5: Adaptive algorithm for noise cancellation

4   Results

In the previous section, it was mentioned that the received signals from each ring are phase shifted in order to superpose their corresponding *T(0,1)* modes on each other. This effect is illustrated in Figure 6-(a) where the two sets of signals, generated using the FEA model using a 10 cycle hann-windowed with frequency of 30 kHz, are shown by red and blue lines. For increasing the energy of the coherent noise in the tests, only source points 1, 7, 14, and 26, which are marked as red in Figure 6-(b), are used as the reception points of the FEA tests.

As mentioned previously, two *T(0,1)* signals must be detected approximately at 3 m and 4 m. Focusing on these regions, one can see the signals from two rings, although does not display exact same amplitude, but are highly correlated and completely in phase with each other. Furthermore, considering the noise region around them, the characteristics of the waves are completely different. In normal routine, the final result is the summation of

these two, but in this work, these two signals are used as the reference and input signals required for adaptive filtering.
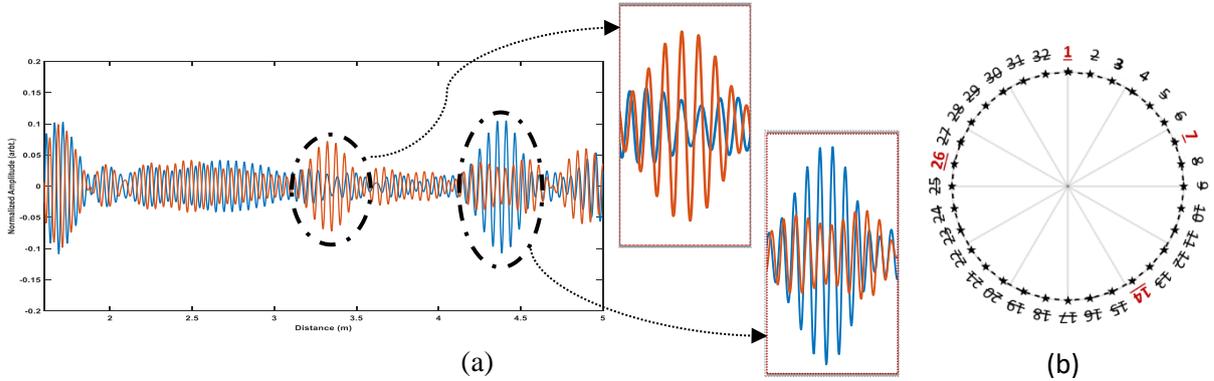

Figure 6: (a) FEA signal from 30kHz excitation frequency with Transfer Functions and non-linear reception. The positions of active receiving points are marked by red in (b).

The filter parameter for in the tests are shown in Table 1. These parameters are selected, by applying a brute force search on FEA model with excitation frequency of 30 kHz in order to find the optimum values which achieves the highest SNR in the test. In these trials, the SNR is defined by the following formula:

$$\text{SNR} = 20 * log10 \left(\frac{1/N \sum_{i=1}^{N} |Signal|}{1/M \sum_{j=1}^{M} |Noise|} \right) \tag{2}$$

where $Signal$ is considered as the $T(0,1)$ signal at 3 m with the length of N, and $Noise$ is considered as everything else (neglecting $T(0,1)$ signal at 4 m) with the length of M.

The excitation waveforms used in these tests is a 10 cycle hann-windowed sine wave with frequency of 30 kHz and 40 kHz. Figure 7 shows the results of each test case where black signal is the result of normal propagation routine and the blue signal is the output of the filter. Cases (a) and (b) are illustrating the signals from FEA model using 30 kHz and 40 kHz excitation frequency respectively. In each case, the detected window of the one in between 3 – 3.5 m which is marked by the two dotted red lines.

Table 1: User inputs to the algorithm

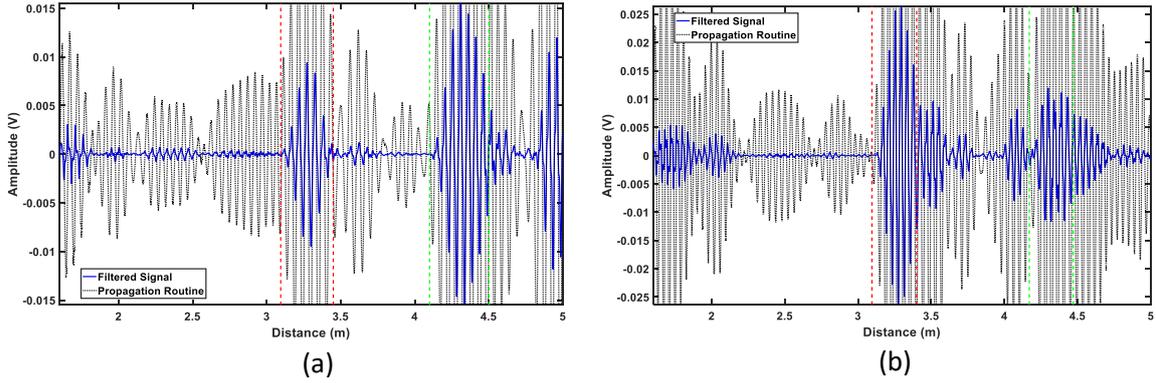| Parameter Name	Symbol	Value
Filter-Order	M	5
Step-Size	β	0.06
Compensation-Factor	ε	0.76
Forgetting Factor	α	0.01

6

Figure 7: The results from tests where black lines are showing the normal propagation routine and blue lines are showing the filtered signals.

Table 2 shows the calculated SNR from the tests. It is demonstrated that adaptive leaky filters are capable of increasing the SNR using the fixed parameters. Both tested frequencies observed an increment of approximately 6 dB. In terms of regional noises caused by high order Flexural waves, significant reduction is observable. As an example, in case (b), significant reduction of Flexurals in the region between 2.1 - 3 m is achieved although the reduction is less for lower order Flexurals in the region between 1.5 – 2.1 m.

Table 2: The SNR from each test showing the Normal Propagation Routine and after Adaptive Filtering.

Excitation Frequency	SNR (dB)		
	Propagation Routine	Filtered Signal	Increment
30kHz	5.89	11.98	6.09
40kHz	7.14	12.75	5.61

5   Conclusion

In the general propagation routine of the system, two sets of signals are created by phase delaying the received signals of the rings in order to have unidirectional reception. As opposed to the propagation routine where the results are the summation of these two sets of signals, in this paper it is suggested to use adaptive filters in order to reduce the coherent noise of the tests. The used adaption algorithm is Leaky Normalized Mean Square (NLMS), as it is providing the capability of forgetting the past filter values in order to adapt itself with the current characteristics of each iteration. This method was validated using synthesised signals created by the FEA. The results demonstrated that this approach is able to enhance the SNR and remove higher order flexurals from the tests. Furthermore, the output of technique can be post-processed using other approaches such as SSP for further enhancement of SNR. Although, fixed parameters of adaptive filter are used which are found by brute force search on the FEA model with 30 kHz. Using the same parameters, the filter was still able to produce higher SNR in the case of 40 kHz excitation frequency. Nonetheless, the dependency of the results with regards to the frequency and filter parameters must be investigated.

6 Acknowledgement

7 References

1. ASTM Standard E2775 - 16, *Standard practice for guided wave testing of above ground steel pipeword using piezoelectric effect transducer*. West Conshohocken, 2017.
2. B. Pavlakovic, "Signal Processing Arrangment," US 2006/0203086 A1, 2006.
3. K. Thornicroft, "Ultrasonic Guided Wave Testing of Pipelines using a Broadband Excitation," Brunel University London, 2015.
4. M. K. Yücel *et al.*, "Coded Waveform Excitation for High-Resolution Ultrasonic Guided Wave Response," *IEEE Trans. Ind. Informatics*, vol. 12, no. 1, pp. 257–266, 2016.
5. S. Fateri, N. V. Boulgouris, A. Wilkinson, W. Balachandran, and T. H. Gan, "Frequency-sweep examination for wave mode identification in multimodal ultrasonic guided wave signal," *IEEE Trans. Ultrason. Ferroelectr. Freq. Control*, vol. 61, no. 9, pp. 1515–1524, 2014.
6. S. Malo, S. Fateri, M. Livadas, C. Mares, and T. Gan, "Wave Mode Discrimination of Coded Ultrasonic Guided Waves using Two-Dimensional Compressed Pulse Analysis," *IEEE Trans. Ultrason. Ferroelectr. Freq. Control*, no. May, pp. 1–10, 2017.
7. S. K. Pedram, S. Fateri, L. Gan, A. Haig, and K. Thornicroft, "Split-spectrum processing technique for SNR enhancement of ultrasonic guided wave," *Ultrasonics*, vol. 83, pp. 48–59, 2018.
8. P. D. Wilcox, "A rapid signal processing technique to remove the effect of dispersion from guided wave signals," *IEEE Trans. Ultrason. Ferroelectr. Freq. Control*, vol. 50, no. 4, pp. 419–427, 2003.
9. R. Guan, Y. Lu, W. Duan, and X. Wang, "Guided waves for damage identification in pipeline structures : A review," *Struct. Control Heal. Monit.*, no. February, pp. 1–17, 2017.
10. M. J. S. Lowe and P. Cawley, "Long Range Guided Wave Inspection Usage – Current Commercial Capabilities and Research Directions," *Imperial College London*, 2006. [Online]. Available: http://www3.imperial.ac.uk/pls/portallive/docs/1/55745699.PDF.
11. A. H. Meitzler, "Mode Coupling Occurring in the Propagation of Elastic Pulses in Wires," *J. Acoust. Soc. Am.*, vol. 33, no. 4, pp. 435–445, 1961.
12. P. Catton, "Long Range Ultrasonic Guided Waves for Pipelines Inspection," Brunel University, 2009.
13. J. Hua and J. L. Rose, "Guided wave inspection penetration power in viscoelastic coated pipes," *Insight Non-Destructive Test. Cond. Monit.*, vol. 52, no. 4, pp. 4–11, 2010.
14. H. Nakhli Mahal, P. Mudge, and A. K. Nandi, "Comparison of coded excitations in the presence of variable transducer transfer functions in ultrasonic guided wave testing of pipelines," in *9th European Workshop on Structural Health Monitoring*, 2018.
15. M. J. S. Lowe, D. N. Alleyne, and P. Cawley, "The Mode Conversion of a Guided Wave by a Part- Circumferential Notch in a Pipe," *J. Appl. Mech.*, vol. 65, no. 649, 1998.
16. Ssanalysis, "Abaqus/Explicit." [Online]. Available: http://www.ssanalysis.co.uk/.
17. M. G. Bellanger, *Adaptive Digital Filters, Revised and Expanded*, Second. New York: Marcel Dekker, Inc, 2001.
18. Y. Zhu and J. P. Weight, "Ultrasonic nondestructive evaluation of highly scattering materials using adaptive filtering and detection," *Ultrason. Ferroelectr. Freq. Control. IEEE Trans.*, vol. 41, no. 1, pp. 26–33, 1994.

19. D. A. Cartes, L. R. Ray, and R. D. Collier, "Experimental evaluation of leaky least-mean-square algorithms for active noise reduction in communication headsets," *J. Acoust. Soc. Am.*, vol. 111, no. 4, pp. 1758–1771, 2002.

20. S. C. Douglas, "Performance Comparison of Two Implementations of the Leaky LMS Adaptive Filter 1 Introduction," vol. 45, pp. 2125–2129, 1997.

21. M. H. Hayes, *Statistical Digital Signal Processing and Modeling*. New york: John Wiley & Sons, Inc., 1997.